Numerical Simulation of Ice Clearing and Jam Initiation in Navigation Channels

Mohamed Sayed[*] and Brian Morse[**]

**National Research Council, Ottawa, Ontario, Canada*
E-mail: Mohamed.Sayed@nrc.ca
*** formerly with the Canadian Coast Guard now with Laval University, Quebec City, Quebec, Canada*
Brian.Morse@gci.ulaval.ca

Abstract

This paper reports on a numerical study of the conditions which may lead to ice jam initiation in navigation channels, such as those of the St. Lawrence Seaway. The numerical model is based on a two-dimensional discrete element formulation. Ice floes inside the channel are modelled as rough inelastic disks. The circular disks are joined at random in groups of two, three and four disks. The resulting realistic irregular shapes can account for the interlocking which may occur between floes. The simulations are done by calculating the contact forces between floes then solving the equations of motion of individual floes. The results give values of ice velocities, flux and concentration. The simulation runs examined the role of channel's width and geometry, water current, and wind. Test runs also addressed cases where large floes and obstacles may be encountered within the channel. The conclusions can thus be used to determine the effective of ice jam prevention strategies.

1. Introduction

Ice jams often occur in a wide section of the St. Lawrence River, about 100 km downstream of Montreal, known as Lake St. Peter. The capacity of the navigation channel to clear ice floes depends on water current, wind and geometry of the channel. When the flux of ice floes exceeds the ice clearing capacity of the channel, ice floes start to accumulate and form a jam. The accumulation of ice floes propagates upstream, and increases in depth. The ice jam may also reduce water current, which in turn would make it more difficult to clear the jam. As floes remain stationary, they may freeze together,

thereby increasing the strength of the jam. For a review of ice jams morphology and historical records in Canada, see Gerard (1990).

Most models of ice jams have so far dealt with the growth and propagation of the jams once they form. Only a few models have dealt with predicting the occurrence of a jam. Early models considered the static equilibrium of "ice bridges" (e.g. Beltaos, 1983, and Flato and Gerard, 1986). That approach takes into account a simple case of Mohr-Coulomb conditions that correspond to the so-called *active* and *passive* stress states. By considering the equilibrium of forces acting on a jam, a formula relating jam thickness to applied drag forces, water surface slope and channel width is obtained. That formula has been widely used and calibrated (e.g. Beltaos, 1988, and Healy et al. 1997).

In many cases, however, the spatial variations of ice conditions may be important. Numerical models are needed for such cases. Shen et al. (1993) used a discrete parcel formulation coupled with a hydrodynamic model to deal with complex geometries. They applied that model to the Grass Island Pool area of the Upper Niagara River. Subsequent enhancements to that model were reported by Shen et al. (1997). Daley and Hopkins (1998) used a discrete element approach to model ice jams. They used a three-dimensional discrete element approach coupled with a one-dimensional hydrodynamic model, thereby allowing the analysis of complex geometries such as river sections constricted by bridge piers.

The present work is based on a two-dimensional discrete element formulation. This approach makes it possible to model complex channel geometries. A two-dimensional model was chosen rather than a three-dimensional one because the horizontal dimensions of the channel are considerably larger than jam thicknesses (by several orders of magnitude. Sayed et al. (1995) gave a description of the formulation of the model. More details on the present study were given by Sayed (1994).

The study area consists of Curve 2 and the downstream straight part of the channel ending at Yamachiche basin of Lake St. Peter. This area is sufficient to examine the role of the various variables that affect ice behaviour (wind, water current and channel's geometry). A larger area was not used at this stage in order to expedite the development of the model and adjusting its parameters. The simulations examine the ice clearing capacity of the channel and the conditions that can initiate the jam. The effects of changing the channel's geometry and water current on ice behaviour are examined.

2. The Model

2.1 Governing equations

Ice floes are modelled as rough, inelastic disks. The circular disks are joined at random in groups of two, three and four disks. The resulting irregular shapes can account for the

interlocking which occurs between ice floes. The total force acting on each floe is the vector sum of wind drag, water drag and contact forces from the other floes. The balance of linear momentum of each floe may be expressed as

$$m\frac{du}{dt} = A\tau_a + A\tau_w + \sum_{i=1}^{n} F_i \tag{1}$$

where m is the mass of the floe, u is the velocity, A is the surface area, τ_a is wind stress. τ_w is water stress and $\Sigma^n_{i=1}F_i$ is the vector sum of contact forces due to n contacts.

$$\begin{aligned} \tau_a &= C_a u_a \\ \tau_w &= C_w(u_w - u) \end{aligned} \tag{2}$$

Wind and water stresses are calculated according to the following linear equations where C_a is the air drag coefficient, C_w is the water drag coefficient, u_a is wind velocity and u_w is water current velocity. These drag equations are considered adequate for the present study.

The balance of angular momentum of a floe is given by

$$I\frac{d\omega}{dt} = \sum_{i=1}^{n} T_i - T_v \tag{3}$$

where I is the moment of inertia of the floe, ω is the angular velocity, $\Sigma^n_{i=1}$ T_i is the sum of torques due to n contacts and T_v is the water drag resisting torque which acts on the bottom of the floe. Nonlinear drag can be used in the simulations, but the linear drag was used for simplicity. It particularly simplifies calculations of the rotational drag, T_v.

2.2 Contact model

When contact occurs between two floes, normal and tangential forces increase as the centres of the floes approach each other. Initial simulations used a spring and a dashpot to model the normal force. This contact model was replaced by another representation of the normal force that is independent of the velocity. The normal force was calculated using linear loading and unloading springs (Fig.1). The loading spring constant, k_1 is larger than the unloading constant k_2. The normal force between two floes would be given by

$$\begin{aligned} loading: \quad & F_n = k_1 \delta \\ unloading: \quad & F_n = k_2 \delta \end{aligned} \tag{4}$$

where δ is the relative normal displacement. Energy dissipation in this case is

proportional to the area within the loading-unloading loop. This energy dissipation is independent of the relative velocity between floes. The tangential force F_s is calculated according to a Coulomb friction law

$$F_s = \mu F_n \tag{5}$$

where μ is the friction coefficient.

2.3 Simulation scheme

Computations are done by keeping track of the positions and velocities of the individual floes. At each time step, the overlap between floes and the contact forces are calculated. Wind and water drag forces are then added. For each floe, the forces are added from the constituent disks. Accelerations are calculated from the resultant forces. Velocities and positions are next determined by numerically integrating the accelerations. The preceding scheme is repeated at each time step. The time step has to be kept small enough such that any contact between floes would span several steps (approximately 50).

The most time consuming part of the simulation is calculating the distances between each disk and all other disks in order to determine contact forces. The computer time needed to calculate those distances is proportional to square of the number of disks. A method traditionally used to reduce running time is to maintain a "neighbours list" for each disk. This method was not effective because of the relatively large number of floes. Another approach was devised by considering a square grid to cover the study area. At each time step, each disk is assigned to a cell according to its position. When calculating contact forces on a floe, only neighbouring cells are considered. This approach considerably speeded the computations. Also running time became linearly proportional to the number of cells, which makes it possible to simulate large numbers of floes.

3. Test Area and Environmental Forces

We consider a section of the navigation channel that starts from upstream of Curve 2 and ends at Yamachiche basin. The total length is 7.5 km. A view of the test area is shown in Fig. 2. The width of the straight channel is 244 m. Curve 2 widens to reach a width of 375 m at the middle. The boundaries of the channel are represented by fixed circular floes; each of 30 m diameter. The drifting floes are modelled as groups of two, three and four disks. Each disk has a diameter of 30 m. In cases of densest packing, as shown in Fig. 2, the total number of disks was 4300 which formed 1400 groups.

The channel was filled with floes prior to starting the simulation runs. This was done by blocking the downstream end of the channel and introducing floes at the upstream end. Those floes moved under water drag forces to fill the channel. The resulting configuration of ice floes was used to start subsequent runs. In some cases, the upstream end was left free. Floes were introduced at the upstream end of the test section in a few

runs. The results obtained using both upstream conditions were similar. Introducing floes upstream, however, results in simulations that cover longer durations.

The downstream end (exit) of the channel was kept free in most cases. The role of an obstruction at the channel's exit was examined in a series of runs. Those obstructions represent, for example, anchored ships in the channel.

Water current was considered to act along the average direction of Curve 2 until the intersection with the straight channel. At that point, water current direction changes to follow the direction of the channel. A water current of 0.5 m/s was used in most runs. In addition, a range of water current values (from 0.3 m/s to 0.9 m/s) was examined. Test runs parameters were chosen in order to examine the role of the following variables:

1- Smoothing the transition between Curve 2 and the straight channel.
2- Changing the channel's width.
3- Water current.
4- Wind magnitude and direction.
5- An obstruction downstream the channel.
6- A single large floe in Curve 2.

4. Results

4.1 Processing of simulation output

The simulations give records of floe positions, rotations, velocities and contact forces. The records from each simulation run were processed to give values of ice velocities, concentration and flux. These values had to be spatially averaged over areas that are sufficiently large to give representative estimates of ice cover behaviour. At each time step, ice floes within two sections, each one-km long, were used to determine the averages. One section was taken in the middle of Curve 2, and the other in the middle of the straight channel. The average velocity component along the x or y direction, <v> is calculated as follows

$$< v >= \frac{\sum_i v^i a^i}{\sum_i a^i} \tag{6}$$

where v^i is the corresponding velocity component (along the x or y direction) of floe i and a^i is the area of the same floe.

The flux (expressed as ice area per unit time) is calculated by taking the average of the area of ice floes which pass the through the cross section of the channel in a unit time. The flux, Q is calculated over each averaging area as

$$Q = \frac{1}{L} \sum_i \left(a^i \, v_x^i \cos\alpha + a^i \, v_y^i \sin\alpha \right) \qquad (7)$$

where L is the length of the averaging section of the channel and α is the angle between the normal to the channel's width and the x-direction.

4.2 Flow patterns

The salient features of ice behaviour are presented here for the *base* case. That case corresponds to the existing geometry of the channel, water current of 0.5 m/s and absent wind. The initial ice concentration is 75%. Because of the circular shape of the disks, the 75% concentration represent a maximum value. That value may be viewed *as completely covered* channel. Animation of floe positions showed that a temporary jam occurred after two hours from starting the simulation, but broke very quickly. Floe positions and velocity vectors after two hours are shown in Figs. 3 and 4, respectively.

The flux, velocity and concentration are plotted versus time in Figs. 5, 6 and 7. These plots show the values obtained from Curve 2 and from the straight channel. Both ice flux and velocity show more fluctuations in Curve 2 than in the straight channel. Ice flux in the channel approaches 50 m^2/s, and the velocity approaches 0.42 m/s. Ice concentration drops from the initial value of 75% to reach approximately 42% in the channel.

Boundary conditions were examined by introducing floes at the upstream end of the test section. Floes were introduced at a flux of 50 m^2/s, which is the average value obtained from the base case. The resulting ice fluxes were almost identical to the base case. Introducing floes upstream, however, makes it possible to simulate longer durations.

4.3 Parametric study

The simulations examined the role of several factors, as mentioned earlier. A few examples of the results are presented here. A complete documentation of the runs is available in a report by Sayed (1994).

For example, geometry of the channel boundary was altered to produce a more gradual and wider transition from Curve 2 to the downstream straight section. This *smoother* transition increases ice flux from 50 m^2/s to 60 m^2/s. Also the jam, which occur with existing geometry, does not form with the smoother curvature. Ice velocity, however, remains the same.

Simulations were done using channel widths of 274 m and 213 m, in addition to the existing channel width of 244 m. The resulting time records of ice flux are compared in Fig. 8. The larger width increases the ice flux to between 60 m^2/s and 70 m^2/s. The smaller width decreases the flux to between 30 m^2/s and 40 m^2/s. Changes in ice velocity, again, were very small.

In addition to the 0.5 m/s water current, the following values were used: 0.3 m/s, 0.7 m/s and 0.9 m/s. The resulting time records of ice velocity are compared in Fig. 9. Increasing the magnitude of water current increases ice flux and velocity. The fluxes corresponding to water currents of: 0.3 m/s, 0.5 m/s, 0.7 m/s and 0.9 m/s are: 35 m^2/s, 50 m^2/s, 60 m^2/s and 70 m^2/s. The corresponding ice velocities are 0.26 m/s, 0.42 m/s, 0.6 m/s and 0.77 m/s. For the 0.5 m/s current, there was a tendency to initiate ice jams, which appeared as intermittent stoppage of ice flow. This behaviour (intermittent flow stoppage) was more pronounced for the 0.3 m/s water current. The faster currents of 0.7 m/s and 0.9 m/s completely prevented the tendency to initiate ice jams.

Runs also examined the effect of a partial obstruction of the channel's exit, and the role of a single large floe in initiating a jam. The results indicate that an obstruction at the exit may cause the ice floes to bridge, and is likely to produce a jam. Also a large floe of an average diameter of 100 m may occasionally initiate a jam, depending on its trajectory in the channel.

5. Conclusions

Ice flux, which represents the ice clearing capacity of the navigation channel, was determined as well as ice velocities and concentrations. Numerical simulations examined the role of the following variables:
- Channel's geometry and width.
- Water current.
- Wind.
- Obstructions in the channel.
- Formation of large individual floes in Curve 2.

The conclusions are:

1. An ice jam may occur if ice flux arriving from upstream exceeds the clearing capacity of the channel or if floes in Curve 2 froze together to form large floes (approximately 100 m diameter or more).

2. The ice clearing capacity is very sensitive to obstructions in the downstream channel (e.g. due to an anchored ship or a floe drifting from the North). Such obstructions substantially reduce the ice clearing capacity and are likely to initiate ice jams.

3. Increasing the navigation channel's width from the present 244 m by 12.5% increased ice clearing capacity by 20%. Decreasing the channel's width by 12.5% reduced ice flux by 34%.

4. Increasing water current increases the ice clearing capacity and diminishes the tendency for jam initiation. Increasing the water current from 0.5 m/s to 0.7 m/s increases

ice flux by 20%. If the current increases to 0.9 m/s (from 0.5 m/s), ice flux increases by 40 %. A decrease of water current from 0.5 m/s to 0.3 m/s, decreases ice flux by 30 %.

5. Wind from the north-east was reduced ice clearing capacity of the channel. For a channel with clear exit, a 7.5 m/s wind from the north-east reduced ice flux from 50 m^2/s to 37 m^2/s (a reduction of 26%). When the channel's exit was partially blocked, a similar wind caused a jam.

As a follow-up to the above study, the model was applied to the same section of the channel, but using a detailed hydrodynamic input. That input accounted for the spatial distribution of water current. The results were reported by Serrer et al. (1997). The trends that emerged from those results are in agreement with those reported above.

Acknowledgements

The support of the Canadian Coast Guard is gratefully acknowledged.

References

Belatos, S. (1983). "River ice jams; theory, case studies, and applications," *J Hydraulic Eng, ASCE*, Vol 109, No. 10, pp 1338-1359.

Belatos, S. (1988). "Configuration and properties of a breakup jam," *Canadian J of Civil Eng*, Vol. 15, pp. 685-697.

Daley, S.F., and Hopkins, M.A. (1998). "Simulation of river ice jams," *Ice in Surface Waters*, Ed. Shen, Balkema Pub, pp. 101-108.

Flato, G.M., and Gerard, R. (1986). "Calculation of ice jam thickness profile," *4th Workshop on Hydraulics of River Ice*, Montreal, June 19-20.

Gerard, R. (1990). "Hydrology of floating ice," *in Northern Hydrology: Canadian Perspective*, ed. T.D. Prowse and C.S.L. Ommanney, NHRI Science Report No. 1, pp 103-134,Environment Canada, 11 Innovation Blvd, Saskatoon, Saskatchewan, Canada S7N 3H5

Healy, D., Hicks, F., and Beltaos, S. (1997)."A comparison of the ICEJAM and RIVJAM ice jam profile models," *the 9th Workshop on River Ice*, September 24-26, Fredericton, N.B., Canada, pp.269-289.

Sayed, M. (1994)."Numerical simulation of ice jams in Lake St.Peter," Technical Report IECE-CRT-CTR-004, National Research Council, Ottawa, Ontario, Canada K1A 0R6, March 1994.

Sayed, M., Neralla, V.R., and Savage, S.B. (1995)."Yield conditions of an assembly of discrete ice floes," *Proc 5th Int Offshore and Polar Eng Conf (ISOPE)*, The Hague, The Netherlands, June 11-16, Vol. 2, pp 330-335.

Shen, H-T, Chen, Y-C., Wake, A. and Crissman, R.D. (1993). "Lagrangian discrete parcel simulation of river ice dynamics," *Proc 3rd Int Offshore and Polar Eng Conf (ISOPE)*, Singapore 6-11 June, Vol. 2, pp 562-566.

Shen, H-T, Lu, S., and Crissman, R.D. (1997). "Numerical simulation of ice transport over the Lake Erie-Niagara River ice boom," *Cold Regions Science and Technology*, Vol. 26, pp. 17-33.

Serrer, M., Sayed, M., Crookshank, N., and Zhang, J. (1997). "Numerical simulation of ice flow at Curve 2, Lake St. Peter," Technical Report HYD-TR-019, National Research Council, Ottawa, Ontario, Canada K1A 0R6, September 1997.

Walton, O.R. and Braun, R.L. (1986). "Viscosity and temperature calculations for assemblies of inelastic frictional disks," *J. Rheology*, Vol. 30, pp. 949-980.

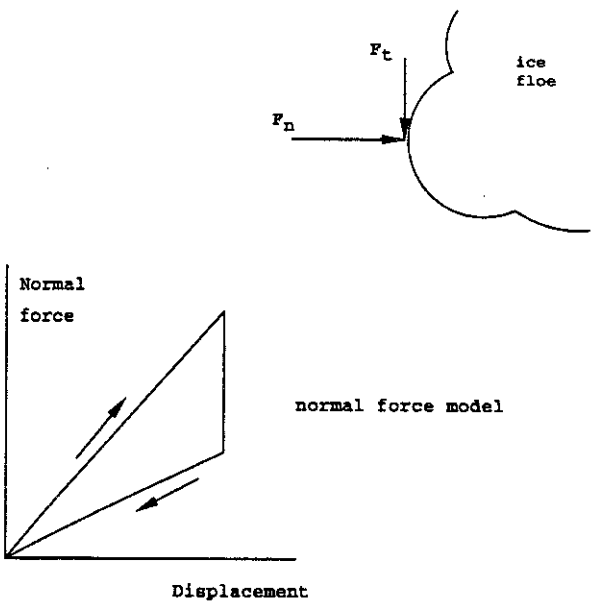

Figure 1: Contact model.

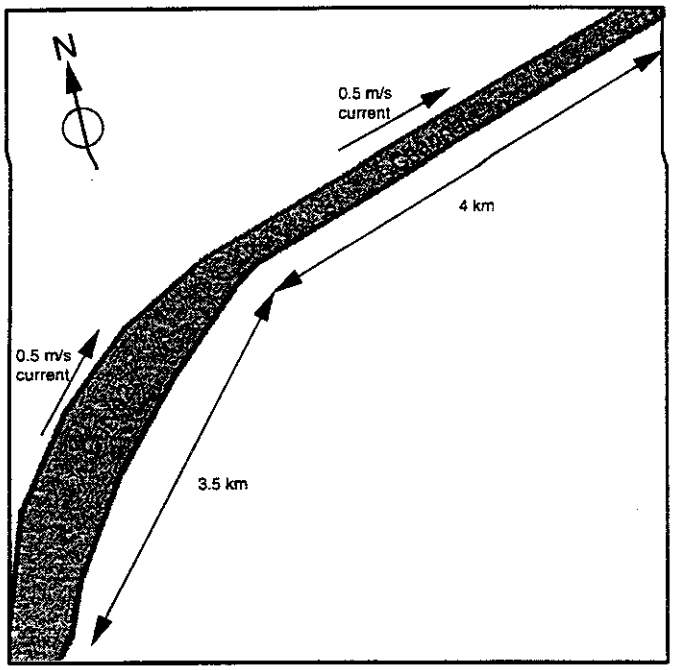

Figure 2: Initial ice floe configuration.

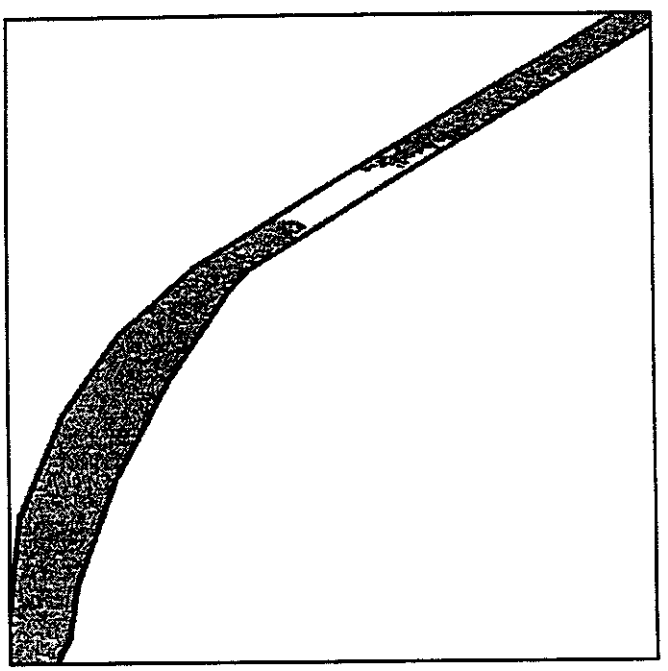

Figure 3: Ice floe positions after 2 hours, base case.

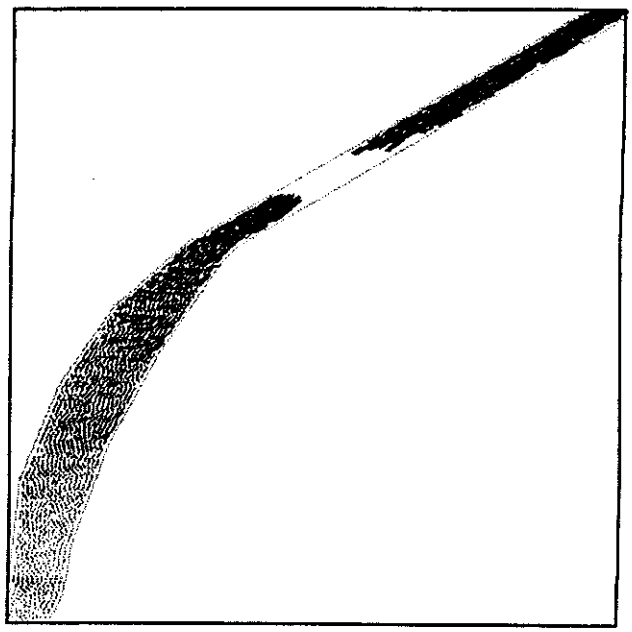

Figure 4: Velocity vectors after 2 hours, base case.

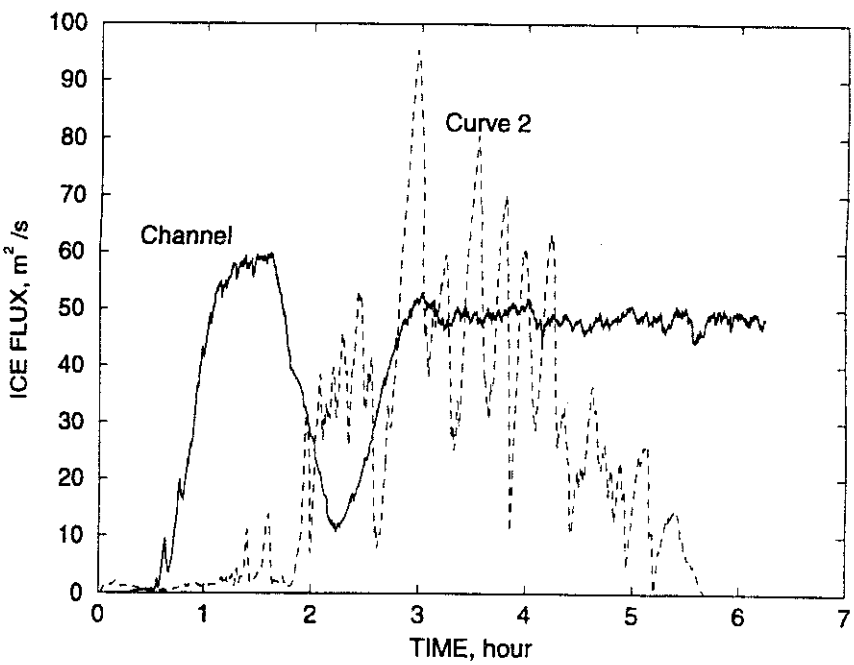

Figure 5: Ice flux versus time, base case.

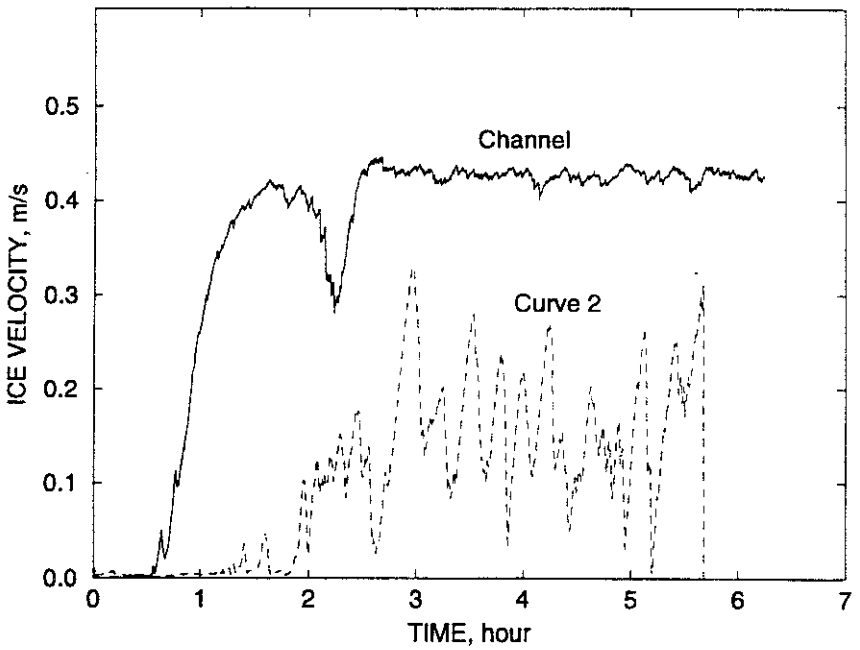

Figure 6: Ice velocity versus time, base case.

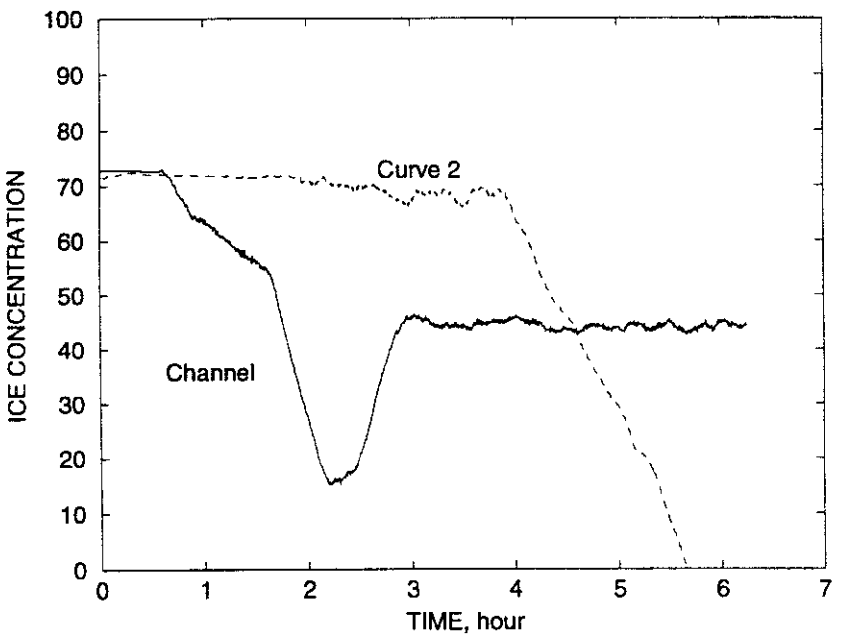

Figure 7: Ice concentration versus time, base case.

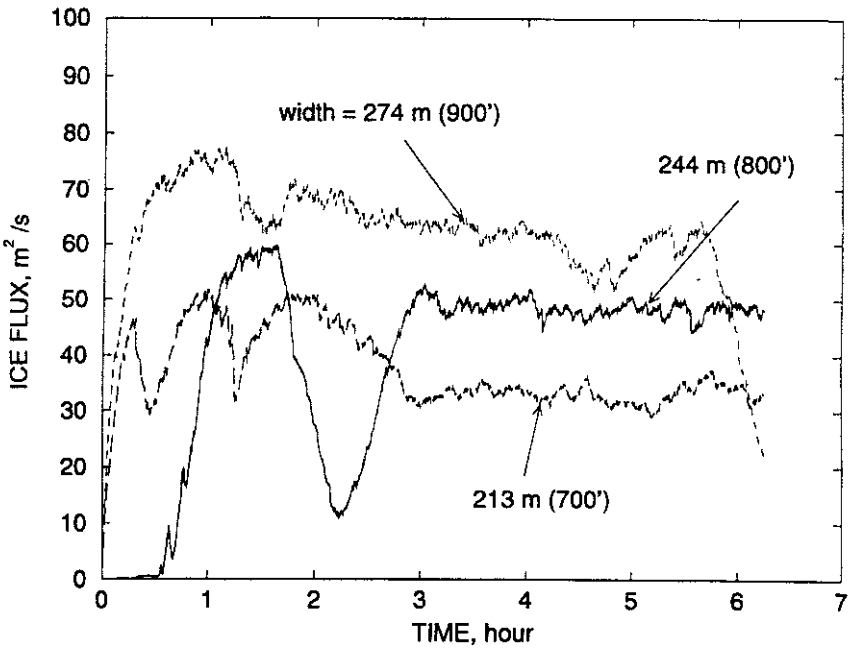

Figure 8: The effect of changing the channel's width on ice flux.

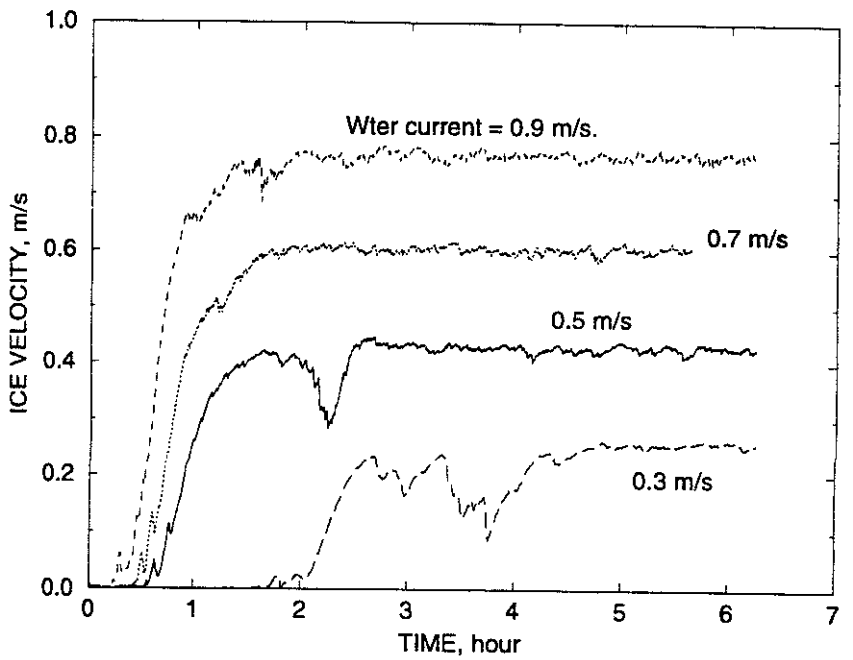

Figure 9: The influence of water current on ice velocity.